Structural Eng./Earthquake Eng., JSCE, Vol. 20, No. 2, 105s—118s, 2003 July
(J. Struct. Mech. Earthquake Eng., JSCE, No. 738/ I —64)

ANALYSIS METHODS OF STOCHASTIC MODEL: APPLICATION TO STRONG MOTION AND FAULT PROBLEMS

Muneo HORI[1], Tsuyoshi ICHIMURA[2] and Hidenori NAKAGAWA[3]

[1] Earthquake Research Institute, University of Tokyo (Yayoi, Bunkyo, Tokyo 113-0032, Japan)
[2] Department of Civil Engineering, Tohoku University (Aoba, Sendai, Miyagi 985-0082, Japan)
[3] Earthquake Research Institute, University of Tokyo (Yayoi, Bunkyo, Tokyo 113-0032, Japan)

The difficulty of modeling underground structures is a bottleneck in quantitatively studying earthquake phenomena. Stochastic modeling that accounts for the uncertainty of modeling is an alternative, and the authors have been developing two analysis methods for a stochastic model. This paper presents these methods in a unified manner, emphasizing the efficiency of numerical computation. The earthquake wave propagation and the surface earthquake fault formation are solved as examples, and the results are compared with observed data to examine the validity and limitation of the analysis methods of the stochastic model.

Key Words : *stochastic modeling, earthquake wave propagation, surface earthquake fault, strong motion, strain localization*

1. INTRODUCTION

Understanding earthquake is indispensable for earthquake engineering, since rational counter measures for earthquake must rely on the soundness of such understanding. As seismology and geophysics are advanced[1),2)], we are able to make more quantitative reproduction or prediction of earthquake phenomena such as strong motion or faulting, both of which cause diverse disasters. While a simple homogenous model is sufficient for qualitative understanding of these phenomena, a more detailed model is required to make more quantitative analysis. However, it is difficult to reliably construct the detailed model, since accurately measuring underground structures, such as geological layers and surface deposits, is not an easy task. In this sense, modeling the underground is a bottleneck in quantitatively studying earthquake phenomena.

An alternative of a deterministic model is a stochastic model[3)]. Here, a deterministic model means a model which has properties and configuration of the underground given in a deterministic manner, while a stochastic model has mean, variance or covariance for parameters of the properties and configurations. Variance or covariance accounts for the uncertainty of the underground that is due to the limitation of measurement. Analyzing such a stochastic model is more laborious; the behavior of the stochastic model becomes stochastic as well. The key issue in analyzing the stochastic model is the fact that

> *the variability of behavior is not necessarily proportional to the variability of model.*

For instance, the variability of the behavior will be magnified if non-linearity is considered for the stochastic model. In dynamic state, there will be cases when the variability is drastically changed since the effects of the spatial variability on various frequency components are different. A Monte-Carlo simulation is usually chosen as an analysis method of the stochastic model. However, it is not suitable for earthquake problems if one simulation requires huge numerical computation.

In order to efficiently analyze a stochastic model, the authors have been developing several analysis methods[4),5),6)]. The developed methods are an extension of analyzing the spatial distribution of heterogeneity to analyzing the spatial and probabilistic distribution; see a monograph[7)] for

a list of the analysis methods for spatially distributed heterogeneity. Two classes of analysis methods are available, the first for evaluating the mean behavior of the stochastic model and the second for efficiently computing the variable behavior of the stochastic model. These two are called the *bounding medium analysis*[4] and the *spectral method*[6], respectively, here.

In this paper, we are aimed at presenting the two analysis methods of the stochastic model in a unified manner. Since they are applied to distinct problems, the two methods are formulated differently and it is not easy to understand that the basic idea of stochastic modeling is common. We pose a stochastic variational problem for a stochastic model and show that the two methods are for solving this problem, i.e., the bounding medium analysis for estimating the mean behavior and the spectral method for computing the full stochastic characteristics of the behavior. The stochastic variational problem will be of interest for those who apply or improve the analysis methods of the stochastic model, which, in our view point, is essential for the quantitative analysis of earthquake phenomena.

The content of this paper is as follows. First, in Section 2, we show the unified formulation of the bounding medium analysis and the spectral method, using the simple two-dimensional problem. Section 3 presents examples of applying the analysis methods to the stochastic model for two earthquake problems, namely, the earthquake wave propagation and the surface earthquake fault formation. Some new results are presented, and they are compared with available data to discuss the validity and limitation of the analysis methods of the stochastic model.

Cartesian coordinates, denoted by x_i, is used. Index notation is used for a vector or tensor quantity, the summation convention is employed, and indices following a comma denote partial differentiation with respect to the corresponding coordinates.

2. FORMULAITON OF ANALYAIS METHODS

For simplicity, we consider a two-dimensional anti-plane shear problem; the formulation presented here is applicable to a more complicated setting such as two-dimensional in-plane problems and three-dimensional problems or even to problems of structural mechanics. We let B be an isotropic but heterogeneous elastic body, and denote by u and c the out-of-plane displacement and the elastic modulus ($u = u_3$ and $c = c_{1313} = c_{2323}$). When, say, boundary displacement $\overline{u}$ is prescribed, the following boundary value problem is posed:

$$\begin{cases} (c(\mathbf{x})u_{,i}(\mathbf{x}))_{,i} = 0 & \text{in } B, \\ u(\mathbf{x}) = \overline{u}(\mathbf{x}) & \text{on } \partial B. \end{cases} \tag{1}$$

This boundary value problem is transformed to a variational problem, in which the stochastic model is more easily treated with. The variational problem uses a functional for u satisfying $u = \overline{u}$ on ∂B,

$$J(u, c) = \int_B \frac{1}{2} c(\mathbf{x}) u_{,i}(\mathbf{x}) u_{,i}(\mathbf{x}) \mathrm{d}s, \tag{2}$$

The solution of Eq. (1), denoted by u^{e}, minimizes J and the minimum value coincides with the total strain energy stored in the body, denoted by E.

We suppose that the elastic modulus c is stochastic, i.e., the value of c at each $\mathbf{x}$ is not given deterministically, but the mean, variance or correlation is provided. To be specific, denoting a stochastic event by ω, we regard c as a random field in $(\Omega, \mathcal{F}, P)$, where Ω is the whole events, $\mathcal{F}$ is Borel sets of ω and P is the probabilistic measure, and put argument ω to emphasize that c is a random field. The displacement $u(\omega)$ that satisfies Eq. (1) for such a stochastic $c(\omega)$ is a random field as well.

(1) Bounding medium analysis

Our first interest is to evaluate the mean of the stochastic displacement that corresponds to the mean behavior of the stochastic model. It should be emphasized that the mean behavior is not the displacement when B has the mean of $c(\omega)$; see later in this subsection. Computing the mean behavior is difficult since the joint probability of $u(\omega)$ and $c(\omega)$ which satisfy Eq. (1) needs to be evaluated. Instead of finding the mean behavior directly, we seek to find certain displacement fields which bound the mean behavior by taking advantage of the *bounding medium theory*[4]. This theory determines two fictitious but deterministic media which provide such bounding displacement fields; see **Fig. 1**.

One bounding medium is determined by using the functional J of Eq. (2). For one realized $c(\omega)$, due to $c(\omega) > 0$, the following inequality holds:

$$E(c(\omega)) = J(u^{\mathrm{e}}(\omega), c(\omega)) \leq J(u, c(\omega)).$$

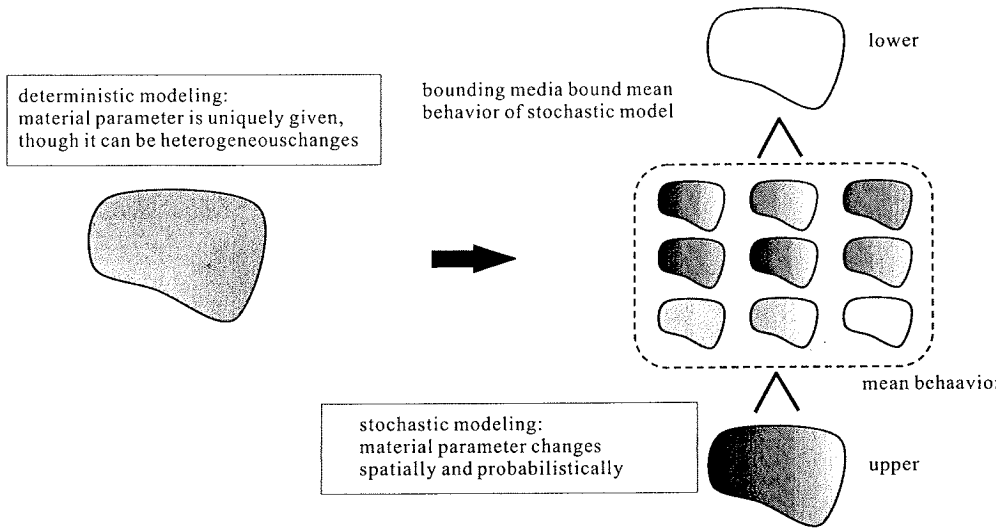

Fig. 1 Bounding medium analysis for stochastic modeling; stochastic models are constructed by probabilistically changing material parameter, and bounding media provide mean behavior of these stochastically generated models.

Here, $u^e(\omega)$ and $E(\omega)$ are the exact solution of the boundary value problem and the total strain energy when $c(\omega)$ is realized. Since $c(\omega)$ is a random field but u is a deterministic, taking the mean for both sides of the above equation, we arrive at

$$\langle E\rangle \leq J(u, \langle c\rangle) \tag{3}$$

for u satisfying $u = \overline{u}$ on ∂B. Here, $\langle(.)\rangle = \int_\Omega (.) P(\mathrm{d}\omega)$ stands for the mean of (.), and the spatial integration and the probabilistic integration are commuted in deriving Eq. (3). The sharpest bound for $\langle E\rangle$ is obtained by the solution of the variational problem that uses $\langle c\rangle$, i.e., displacement of a deterministic body that has the mean elasticity $\langle c\rangle$. Thus, in the sense that an upper bound for the mean total strain energy is given, this fictitious but deterministic body is a bounding medium which overestimates the mean behavior of the stochastic body. It should be noted that the mean elastic modulus, $\langle c\rangle$, does not give the mean behavior since $\langle c\rangle$ overestimates the mean total strain energy.

Another bounding medium is determined by considering the complementary strain energy. We define a functional for stress σ_i as

$$I(\sigma, 1/c) = -\int_B \frac{1}{2c(\mathbf{x})}\sigma_i(\mathbf{x})\sigma_i(\mathbf{x}) + \lambda(\mathbf{x})\sigma_{i,i}(\mathbf{x})\mathrm{d}s + \int_{\partial B} n_i(\mathbf{x})\sigma_i(\mathbf{x})\overline{u}(\mathbf{x})\mathrm{d}\ell, \tag{4}$$

where λ is the Lagrange multipliers which enforce the equilibrium and n_i is the outer unit normal of the boundary. Note that the first variation of I is

$$\delta I = \int_B \delta\sigma_i(\sigma_i/c - \lambda_{,i})\mathrm{d}s + \int_{\partial B} n_i\delta\sigma_i(\lambda - \overline{u})\mathrm{d}\ell,$$

and hence it is required that strain given by σ_i/c is compatible and λ coincides with the exact displacement u^e. In the same manner as for J, the following inequality is derived for I with stochastic $c(\omega)$:

$$\langle E\rangle \geq I(\sigma, \langle 1/c\rangle), \tag{5}$$

since the maximum value of I with $1/c(\omega)$ coincides with $E(\omega)$. The sharpest lower bound for $\langle E\rangle$ is obtained for stress that minimizes $I(\sigma, \langle 1/c\rangle)$. Thus, Eq. (5) shows that a fictitious but deterministic body with $c = 1/\langle 1/c\rangle$ is another bounding medium in the sense that the mean total strain energy is underestimated.

The bounding medium analysis uses the two bounding media to estimate the mean behavior of the stochastic model. The difference of the two bounding media corresponds to the uncertainty of the stochastic model, i.e., as the uncertainty becomes larger, the bounding media behave more differently. It should be mentioned that the bounding medium analysis is an extension of analyzing heterogeneous materials; the elastic moduli of the bounding media, $\langle c\rangle$ and $1/\langle 1/c\rangle$, correspond to the Voigt and Ruess bounds[7] for the effective moduli if the mean is replaced by the volume average. Sharper bounding media can be

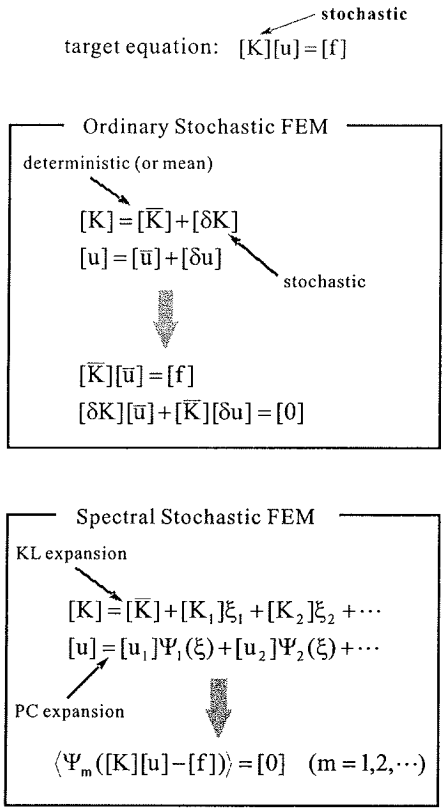

Fig. 2 Comparison of spectral stochastic finite element method with ordinary stochastic finite element method.

constructed if other analysis methods of the heterogeneous materials are used; see Appendix A for the case of the Hashin-Shtrikman variational principle.

(2) Spectral method

Our second interest is to fully evaluate a random field $u(\omega)$ which describes the variable responses of the stochastic model. As mentioned, the difficulty of solving Eq. (1) lies in the evaluation of the joint probability of $c(\omega)$ and $u(\omega)$. Instead of Eq. (1), we transform a variational problem given by Eq. (2) to a stochastic variational problem, such that a correct random field will be obtained just by minimizing the functional without considering the joint probability. To this end, we take the following weak form of the governing equation of $u(\omega)$:

$$\int_B \int_\Omega \delta u(\mathbf{x},\omega)\left(c(\mathbf{x},\omega)u_{,i}(\mathbf{x},\omega)\right)_{,i} \mathrm{d}sP(\mathrm{d}\omega) = 0,$$

where $\delta u(\omega)$ is an arbitrary random field satisfying $\delta u(\omega) = 0$ on ∂S. The probabilistic integration is carried out since $u(\omega)$ is a random field. Integration by part leads to the following stochastic functional for $u(\omega)$ satisfying $u(\omega) = \overline{u}$ on ∂B:

$$J^\omega(u(\omega), c(\omega)) = \int_B \int_\Omega \frac{1}{2} c(\mathbf{x},\omega)u_{,i}(\mathbf{x},\omega)u_{,i}(\mathbf{x},\omega)\mathrm{d}sP(\mathrm{d}\omega). \quad (6)$$

This J^ω gives a stochastic variational problem for a stochastic model of B. It immediately follows from $c(\omega) > 0$ that the random field that minimizes J^ω is the solution of the stochastic model. The joint probability of $u(\omega)$ and $c(\omega)$ does not have to be considered in minimizing J^ω. The joint probability will be automatically computed when the solution of the variational problem is found; see later in this subsection.

The spectral method of Ghanem and Spanos[3] is applicable to solve a variational problem of J^ω. The advantage of this method is that a random filed is expanded in a probabilistic space, just like the Fourier series expansion. Unlike the Fourier series expansion, however, the expansion in the probabilistic space is abstract and does have physical values, except that the probabilistic moments such as mean and variance are computed, which is sufficient in solving a stochastic problem. We present the formulation of the spectral method which is slightly different from the original formulation[6),8),9)]. For simplicity, we consider a case when $c(\omega)$ is a Gaussian random distribution and the covariance function

$$r(\mathbf{x},\mathbf{y}) = \int_\Omega c(\mathbf{x},\omega)c(\mathbf{y},\omega)P(\mathrm{d}\omega)$$

is given. It is shown[3] that $c(\omega)$ admits the following Karhunen-Loeve (KL) expansion:

$$c(\mathbf{x},\omega) = \sum_{n=0} \lambda^n \phi^n(\mathbf{x})\xi^n(\omega), \quad (7)$$

where $\{(\lambda^n)^2, \phi^n\}$ are the eigen-values and eigenfunctions of r,

$$(\lambda^n)^2\phi^n(\mathbf{x}) = \int_B r(\mathbf{x},\mathbf{y})\phi^n(\mathbf{y})\mathrm{d}s_\mathbf{y},$$

and ξ^n is formally given as

$$\lambda^n\xi^n(\omega) = \int_B c(\mathbf{x},\omega)\phi^n(\mathbf{x})\mathrm{d}s_\mathbf{x}.$$

Both ϕ^0 and ξ^0 are uniform in B and Ω, respectively, the mean of ξ^n is zero, and $\{\xi^n\}$ is the

orthonormal complete system of Gaussian distributions in Ω. The base for non-Gaussian random distributions in Ω is constructed by using the polynomial chaos (or the multi-dimensional Hermit polynomials) of $\{\xi^n\}$. That is, for a k-th dimensional vector of $(\xi^{m_1}, \xi^{m_2}, \cdots, \xi^{m_k})$, we define

$$\Gamma_k = (-1)^k \frac{1}{\gamma^k(\{\xi_{m_k}\})} \frac{\partial^k \gamma^k(\{\xi_{m_k}\})}{\partial \xi^{m_1} \cdots \partial \xi^{m_k}},$$

with $\gamma^k = \exp(-\frac{1}{2}\sum_p (\xi^{m_p})^2)$. A group of Γ_k's which are computed by using various ξ^n's and order k is the base for non-Gaussian distributions and denoted by $\{\Psi^m\}$; for instance, Ψ^0 is uniform and Ψ^n coincides with $\gamma^1(\xi^n) = \xi^n$.

The random field $u(\omega)$ is now expanded in the following polynomial chaos (PC) expansion:

$$u(\mathbf{x}, \omega) = \sum_{m=0} u^m(\mathbf{x}) \Psi^m(\omega). \tag{8}$$

When Eq. (7) is truncated up to $n = N$ and the K-th order polynomials is taken, the PC expansion ends up to $M = 1 + \sum_{n=1}^{K} 1/n! \, \Pi_{p=0}^{n-1}(N+p)$. Substituting Eqs. (7) and (8) into J^ω of Eq. (6), we arrive at

$$J^\omega = \sum_{m,m'} \int_B \frac{1}{2} c^{mm'}(\mathbf{x}) u^m_{,i}(\mathbf{x}) u^{m'}_{,i}(\mathbf{x}) \mathrm{d}s_{\mathbf{x}}, \tag{9}$$

where $c^{mm'}(\mathbf{x}) = \sum_n \lambda^n \phi^n(\mathbf{x}) \langle \xi^n \Psi^m \Psi^{m'} \rangle$; the mean of $\xi^n \Psi^m \Psi^{m'}$ is computable since Ψ^m's are given by computable ξ^n's. The boundary conditions for u^m's are derived from $u = \overline{u}$, and we can pose the following boundary value problem for the expanded coefficients $\{u^m\}$:

$$\begin{cases} \sum_{m'=0}^{M} (c^{mm'}(\mathbf{x}) u^{m'}_{,i}(\mathbf{x}))_{,i} = 0 & \text{in } B, \\ u^m(\mathbf{x}) = \overline{u}(\mathbf{x}) \langle \Psi^m \rangle & \text{on } \partial B, \end{cases} \tag{10}$$

for $m = 0, 1, \cdots, M$.

Equation (10) is numerically solved by spatially discretizing u^m. This is the spectral stochastic finite element method[3]. When the coefficients u^m's are determined, the joint probability between $c(\omega)$ and $u(\omega)$ can be computed since they are expanded in $\{\xi^n\}$ and $\{\Psi^m\}$. It should be mentioned that the spectral stochastic finite element method is different from an ordinary stochastic finite element method which takes perturbation for stochastic parts assuming that the stochastic parts are smaller than deterministic parts; see **Fig. 2** for the comparison of the spectral stochastic finite element method with the ordinary one.

In closing this section, we point out that the bounding medium analysis and the spectral method are for solving the stochastic variational problem of J^ω of Eq. (6). If a deterministic function is used, J^ω leads to the (upper) bounding medium, and one deterministic response which overestimates the mean response is obtained. The spectral method solves the stochastic variational problem by expanding random functions in J^ω, i.e., $c(\omega)$ and $u(\omega)$. For a common stochastic model, therefore, we can regard the bounding media analysis as a method to estimate the expectation of the responses and the spectral method as a method to approximately but fully obtain the stochastic characteristics of the responses.

3. APPLICATION TO EARTHQUAKE PROBLEMS

Now, we present examples of applying the stochastic model to earthquake problems and solving the problem with the aid of the bounding medium analysis and the spectral method. Three-dimensional setting is considered. For simplicity, we assume that the undergrounds are stochastic but isotropic; Young's modulus is heterogeneous and stochastic although Poisson's ratio is deterministic and uniform. Symbolic c is now used to denote Young's modulus.

For the bounding medium analysis, we determine bounding media by replacing $cu_{,i}u_{,i}$ in J of Eq. (2) with $ch_{ijkl}u_{i,j}u_{k,l}$, where h_{ijkl} is a constant forth-order tensor given by Poisson's ratio. The elasticity tensor of the bounding media is

$$\langle c \rangle h_{ijkl} \quad \text{and} \quad 1/(\langle 1/c \rangle) h_{ijkl}.$$

For the spectral method, taking the PC expansion of $c(\omega)$ and the KL expansion of $u_i(\omega)$, we can derive boundary value problems for the coefficient u_i^m's

$$\begin{cases} \sum_{m'=0}^{M} (c^{mm'}(\mathbf{x}) h_{ijkl} u^{m'}_{k,l}(\mathbf{x}))_{,i} = 0 & \text{in } B, \\ u_i^m(\mathbf{x}) = \overline{u}_i(\mathbf{x}) \langle \Psi^m \rangle & \text{on } \partial B, \end{cases}$$

for $m = 0, 1, \cdots, M$. In taking the KL expansion, we consider a case when the covariance is expressed in terms of the correlation length L as $\sigma \exp(-\sum_p (x_p - y_p)/L)$ where σ is the variance. The KL expansion is carried out numeri-

Table 1 Characteristics of target earthquakes.

a) epicenter

	Date	Lat.	Long.	Depth
case1	08/11/1999	35.4N	139.8E	53km
case2	05/28/1999	35.5N	139.5E	38km

b) properties

	Strike	Dip	Rake	Mag.
case1	62^o	85^o	73^o	4.0Mw
case2	283^o	70^o	112^o	3.5Mw

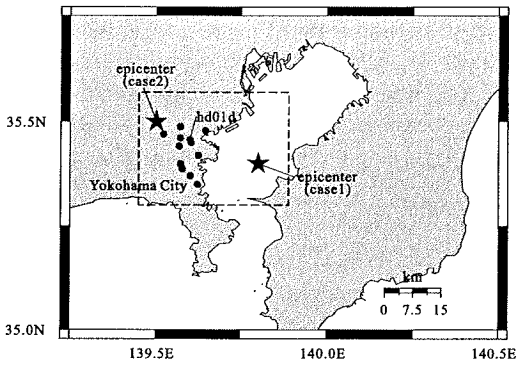

Fig. 3 Epicenter of simulated earthquakes and location of measurement sites.

cally, by solving the discretized equation of $\lambda^2\phi = \int \sigma \exp(-\sum_p (x_p - y_p)/L)\phi \mathrm{d}s$ with $\int \phi^2 \mathrm{d}s = 1$.

(1) Simulation of earthquake wave propagation

As the first example, we consider the earthquake wave propagation; see recent advancement of seismology[10),11),12),13),14)] for computing the wave propagation process; see also related works[15),16),17),18),19),20)]. The underground structures consist of several geological layers which are not necessarily stratified, and it is not realistic to assume that these structures are accurately measured. Thus, stochastic modeling is an alternative of deterministic modeling, i.e., the mean and variance are given to material properties of each geological layer, as well as the location of the interfaces between two layers.

The two bounding media are defined from the stochastic model. For a given focal mechanisms, these media provide estimates for the mean wave that propagates in the stochastic model, i.e., the earthquake wave that is most likely to occur. It should be recalled that the bounding media are defined such that the total strain energy is bounded. The behavior of the bounding media cannot provide bounds for local dynamic responses, such as waveforms, peak ground motions, or some seismic intensities. However, the behavior of the two media becomes closer to each other as the variability of the stochastic model becomes smaller. Therefore, we can expect that the average of the behavior of the two bounding media will be an estimate of the mean behavior and that the difference in the behavior of the two bounding media will be a measure of the uncertainty in the mean behavior due to the variability of the stochastic model. Since this interpretation is naive, the behavior of the bounding media is called *optimistic* and *pessimistic* estimates of the mean behavior.

For engineering purposes, the spatial resolution of the order of, say, 1[m] is needed for the underground structure model to estimate higher wave frequency components of the order of $1 \sim 10$[Hz], since these components have shorter wave length. The length scale of modeling the heterogeneity is much smaller than the length scale of the wave path that connects the fault and a target structure. Thus, the bounding media will have wild change in the elasticity, especially near the ground surface. To solve a highly heterogeneous body problem, we apply the *macro-micro analysis method*[5)] or the multi-scale analysis based on the singular perturbation expansion. The macro-micro analysis method sequentially computes the wave propagation in the geological length scale (macro-analysis) and the wave amplification near the surface (micro-analysis). The micro analysis is capable to compute non-linear responses[5)] of surface layers.

While the macro-micro analysis method is rigorous, it results in an ordinary analysis of computing dynamic ground responses when input wave is given to the bed rock mass. However, there is one major difference that the macro-micro analysis method inputs the wave of the macro-analysis to the whole surface layers. Inputting macro-analysis solution to the surface layers is the same as the dynamic analysis of structural responses in which ground motion is input to all elements of the structure, not only to its foundation nor footing. The macro-micro analysis method also accounts for the effects of the surface layers on the wave propagation; the surface layers are homogenized in modeling the crust structures, and this influences higher frequency wave components when the whole crust structures are densely discretized.

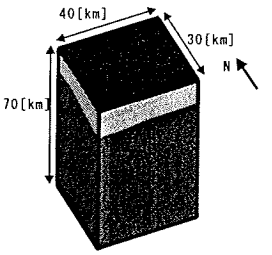

	1	2	3	4
α [m/sec]	1040	1730	2950	5200
β [m/sec]	600	1000	1700	3000
ρ [kg/m^3]	1800	2000	2300	2500

a) analysis domain

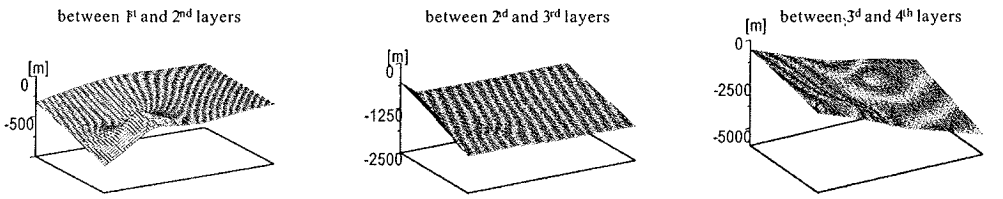

b) interface configuration

Fig. 4 Model for macro-analysis method.

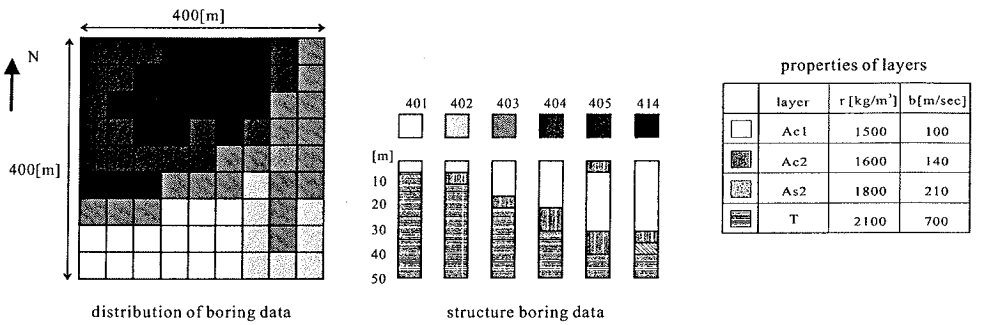

properties of layers

	layer	r [kg/m^3]	b[m/sec]
	Ac1	1500	100
	Ac2	1600	140
	As2	1800	210
	T	2100	700

a) data for ground structure

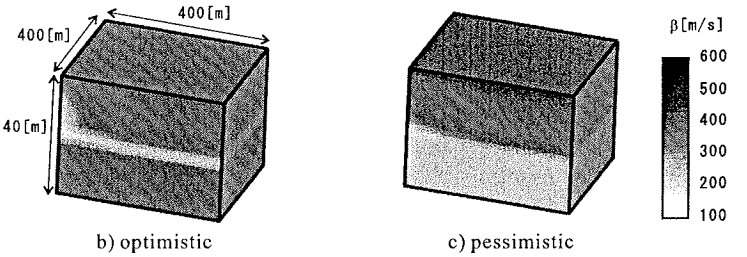

b) optimistic c) pessimistic

Fig. 5 Example of model for micro-analysis method.

High frequency wave components, say, > 1[Hz], must be estimated for engineering purposes. However, it is still difficult to determine such higher wave components through the numerical computation of the wave propagating from the fault. The major reasons of this difficulty are the following two: 1) information on the focal mechanisms that emits high wave components is limited; and 2) discretization needed for the computation is beyond the capacity of high-class computers. In the current macro-micro analysis method, we apply the stochastic Green function

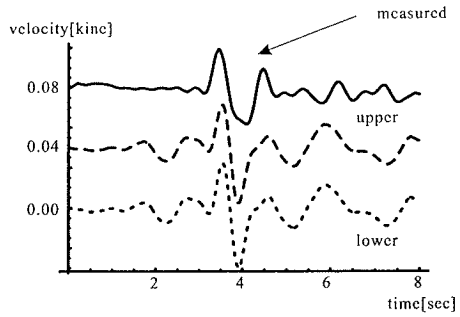

a) case 1

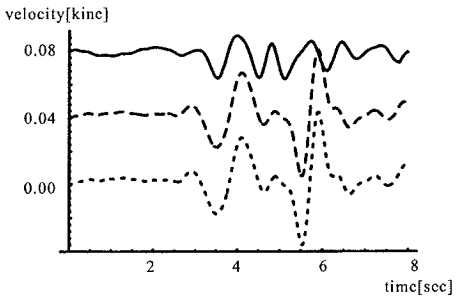

b) case 2

Fig. 6 Comparison of velocity wave form.

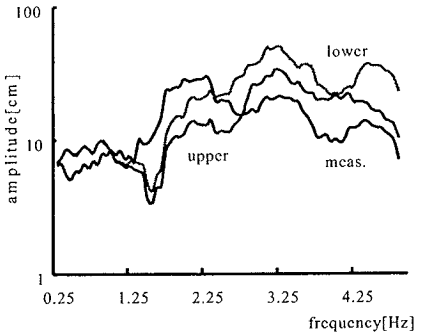

a) NS

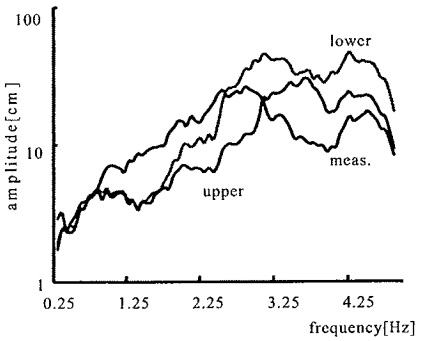

b) EW

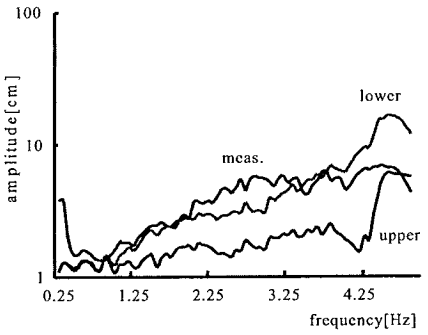

c) UD

Fig. 7 Comparison of velocity spectral.

method, which extrapolates lower frequency components to higher ones using the probabilistic assemble of previous events; note that the stochastic Green function is different from the empirical Green function[21] that uses the past record of the target site.

We carry out numerical simulation of the earthquake wave propagation applying the macro-micro analysis method to the bounding media of the stochastic model[5]. Two earthquakes which occurred near Yokohama City are simulated; see **Fig. 3**. The characteristics of the target earthquakes are shown in **Table 1**. The focal mechanism uses simple rump functions[22]. The three-dimensional model for the macro-analysis method, which consists of four layers, is presented in **Fig. 4**; there are four distinct geological layers[24], and the properties and interfaces are shown in a) and b), respectively. Examples of models for the micro-analysis method are presented in **Fig. 5**; a) presents the 40[m] mesh data stored in a GIS provided by Yokoyama City, and b) and c) are the pessimistic and optimistic models which are constructed by connecting mesh data and computing the bounding media. The GIS stores 40[m] mesh boring data of soil layers down to engineering rock mass together with layer properties; see the reference[5] for the detailed explanation of these data. The difference of the two bounding media is negligible in the geological length scale, and only one model is used for the macro-analysis. The two media are quite different in the length scale of the surface soil layers, as shown in **Fig. 5**. The numerical computation of the micro-analysis uses spatial discretization of 2[m], and hence frequency components up to

5[Hz] are accurately computed.

The target earthquakes were measured at several sites of Yokohama City Seismograph Network; see **Fig. 3**. The results of the numerical simulation are compared with the measured data. For site hd01d, **Fig. 6** shows the comparison of the velocity waveform of the EW component; frequency components higher than 5[Hz] are filtered out in the measured data. In **Fig. 7**, the velocity spectral of the three components is compared. The synthesized waveforms do not bound the measured waveform. This is natural since the bounding media are defined such that the overall strain energy is bounded, we cannot expect that the media provide bounds for local responses. However, the synthesized waves produce similar waveform and spectral. In particular, the similarity in the spectral up to high frequency (4[Hz]) cannot be overlooked. This similarity suggests the bounding media defined for a stochastic underground model serve as an alternative of a deterministic model for uncertain ground structures, in order to estimate the possible strong motion. **Figure 8** presents the comparison of the peak ground velocity. The bounding media do not provide bounds for the measured data, although they are close to the measured values at most of sites. The estimation is quite different from the measured data at two sites; see the data of sites 4 and 10. This is mainly due to the local topographical effects[23] which the stochastic model fails to capture and due to the simple focal mechanism that is used in the macro-analysis. These two are the limitation of the current macro-micro analysis method.

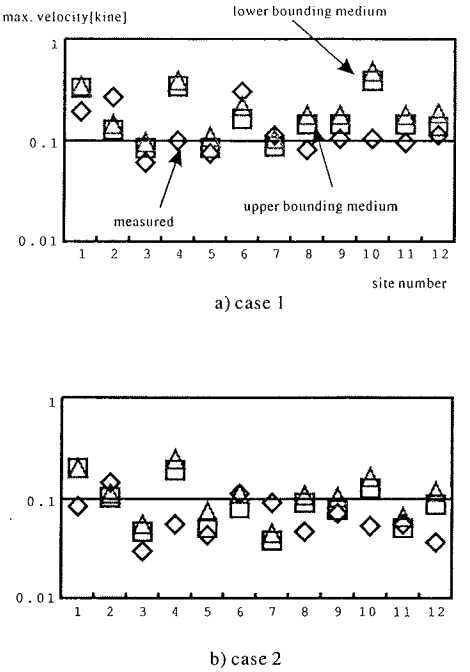

Fig. 8 Comparison of peak ground velocity.

(2) Simulation of surface earthquake fault formation

The second example is the formation of surface earthquake fault; see Konagai[25] for a concise list of recent achievements on the fault problems. For a large earthquake, rupture process on the source fault reaches the ground surface, forming a surface earthquake fault; see numerical researches[26),27),28),29)] and experiment and field researches[30),31)]; see also related works[32),33)]. Echelon fault, a periodic array of oblique cracks caused by lateral sliding, is a typical example of the surface earthquake fault. Large variability in fault displacement is often observed for echelon faults, which is mainly due to the complicated soil layers and the bifurcation during the formation processes[34)]. For engineering purpose, the evaluation of the variability is important for considering rational remedial measures against surface earthquake faults. The variability is numerically computed for the stochastic model of soft surface deposits, by analyzing the echelon fault formation when the bed rock mass slides[6),35),36)].

Since the surface deposits are softer and more ductile than the base rock mass, they are modeled as elasto-plastic materials such that fault is modeled as the accumulation of plastic shear strain. A Mohr-Column type yield function is employed to account for the confining pressure effects on the plastic deformation, i.e., a yield function is given as

$$f = \tau - (f_o + \tan\phi\sigma)$$

where τ and σ are the maximum shear and the confining pressure, and f_o and ϕ are the cohesion and the internal friction angle. Stochastic modeling is applied to the elasto-plastic surface layers; only Young's modulus c is stochastic and deterministic values are given to other material parameters such as Poisson's ratio, the cohesion and the internal friction angle.

For the evaluation of the variability, we seek to find a random field $u_i(\omega)$ in this stochastic and non-linear elasto-plastic body. In incremen-

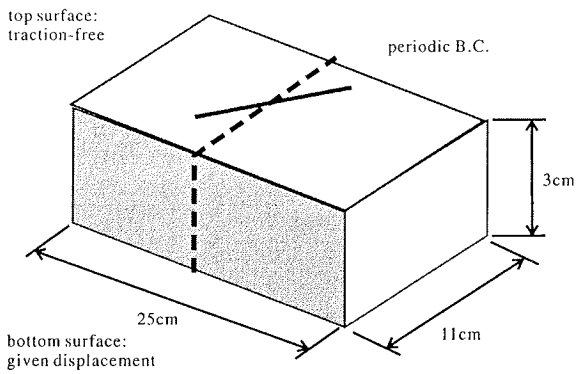

model dimension and boundary conditions

material properties

mean of c [Pa]	1.25
Poisson's ratio	0.25
friction angle [degree]	51
standard deviation of c [Pa]	0.015
corelation length of c [cm]	50

Fig. 9 Characteristics of model experiment and numerical simulation.

tal form, the governing equation of $u_i(\omega)$ is given as

$$(c^{ep}_{ijkl}(\mathbf{x},\omega)\dot{u}_{k,l}(\mathbf{x},\omega))_{,i} = 0, \qquad (11)$$

where $\dot{u}_i$ is displacement increment and c^{ep}_{ijkl} is instantaneous moduli defined as

$$c^{ep}_{ijkl} = \begin{cases} c\left(h_{ijkl} - \dfrac{h_{ijpq}\nabla f_{pq} h_{klrs}\nabla f_{rs}}{\nabla f_{pq} h_{pqrs}\nabla f_{rs}}\right) & f = 0 \ \&\ \dot{f} = 0, \\ c\ h_{ijkl} & \text{otherwise.} \end{cases} \qquad (12)$$

with $\nabla f_{ij} = \partial f/\partial\sigma_{ij}$.

In Eq. (11), both c and f are stochastic, and hence computing c^{ep}_{ijkl} given by Eq. (12) is laborious; the joint probability of c and f needs to be evaluated to compute c^{ep}_{ijkl}. We approximate[6] the stochastic f as deterministic, and stress in the bounding medium is used to compute the deterministic f. This approximation means that the perturbation expansion of the stochastic f is taken at the mean stress and that the mean stress is approximated as stress in the bounding medium. Hence, the approximate solution approaches the exact one as the variability of c decreases; the accuracy of the approximate solution will be higher as the variability in stress becomes smaller. Although this is approximation, Eq. (11) yields a linear stochastic problem for $\dot{u}_i(\omega)$ with stochastic $c^{ep}_{ijkl}(\omega)$. This linear stochastic problem is solved by applying the spectral method.

The spectral stochastic finite element, which computes the boundary value problem of the expansion coefficients in the same manner as an ordinary non-linear finite element method, is developed for this purpose. The validity of this numerical method is verified[6),8] from the comparison with the Monte-Carlo simulation. Thus, the stochastic behavior of the non-linear elasto-plastic body can be evaluated even though it includes some approximation. Relatively laborious numerical computation is required for the spectral stochastic finite element method; one node uses large degree-of-freedoms as the degrees correspond to the expansion coefficients u^m_i for $m = 1, 2, \ldots, M$.

Table 2 Comparison of echelon fault configuration.

	experiment	simulation
orientation of fault direction	26cm	27.9cm
base slip causing failure	5cm	5.2cm
interval between adjacent fault	11cm	11±1cm

For quantitative evaluation, we carry out numerical simulation of a model experiment of echelon faults and compare the results with available data. The model experiment uses sands, and Riedel shears appearing on the surface are a model of echelon faults; **Fig. 9** summarizes the characteristics of the model experiment and the numerical simulation. First, we plot in **Fig. 10** the distribution of the mean and standard deviation for the maximum shear strain on the top surface when the plastic deformation reaches the top surface. Oblique Riedel shears are reproduced in the mean distribution, even though uniform sliding is applied on the bottom surface. The variability in the location of the Riedel shear can be estimated from the standard deviation distribution. The configuration of the computed Riedel shears is compared with the observed ones in **Table 2**. The agreement of the configuration appears fair.

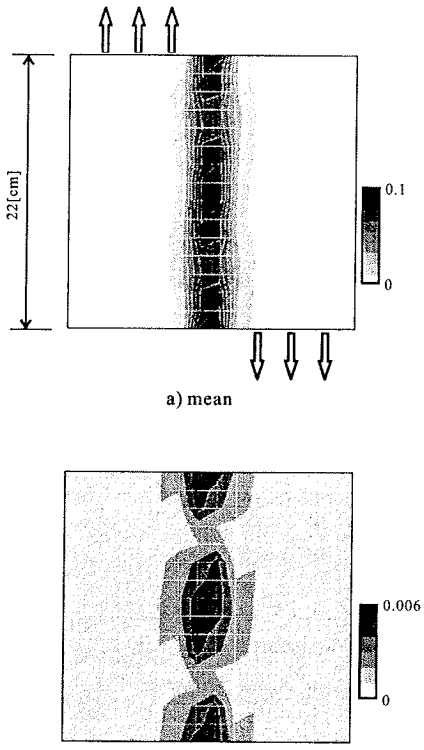

Fig. 10 Examples of echelon fault formation on surface with its variability.

However, we should mention that the numerical simulation does not fully reproduce Riedel shears. In forming Riedel shears, a so-called *embolic* or flower structure is developed from the bottom, in which Riedel shears grow overlapping each other like flow lips. In **Fig. 11**, we present the maximum shear strain distribution on several horizontal planes. As is seen, the computed Riedel shears are evolved without overlapping each other, which does not correspond to the actual Riedel shears. The current numerical simulation cannot reproduce the embolic structure mainly due to the lack in sufficient discretization of the interface between the sliding base and the layers at which Riedel shears are initiated. The usage of simple constitutive relations, as well as the assumption of infinitesimal small deformation and the quasi-static state, may contribute. Further improvement of the numerical computation is required, although it is not easy since the stochastic finite element method sets large degree-of-freedom for nodes.

Admitting the limitation of the numerical simulation, we compute the probability of failure to examine the accuracy of estimating the variability. Here, the failure is defined as the appearance of Riedel shears on the top surface, and, in the numerical simulation, the failure is regarded as the sudden increase in the maximum shear strain on the top surface as the base slip gradually increases. The sudden increase of the maximum shear strain takes place when it approximately attains a critical value of 55%. The probability of failure is given as a function for the amount of the base slip, and is numerically computed through the following procedures: 1) compute the probability density function of the maximum shear on the surface; 2) compute the probability that the maximum shear exceeds the critical value; and 3) differentiate it to derive the probability density function of the failure. The probability density function for failure is plotted in **Fig. 12**. The form of the function is relatively complicated, not like Gaussian nor Poisson distribution. This suggests the complexity in the probabilistic processes[8] of the Riedel shear formation; recall that the source of the variability is the Young modulus that obeys a Gaussian distribution. The mean and standard deviation of the base slip at the failure are calculated from the experimental data, and they are plotted in **Fig. 12**. While the variability given by the standard deviation is underestimated, the mean is well reproduced in the simulation. The variability estimation may be improved if the definition of failure is changed, although this is out of scope of the current paper.

4. CONCULDING REMARKS

In this paper, we present the two analysis methods, the bonding medium analysis and the spectral method, for stochastic models of earthquake problems. These methods are rigorously formulated in the same manner as for the deterministic case; the stochastic variational problem that uses the integration of the strain energy in the stochastic space is a key for the formulation. While only limited comparison is made at this stage, the numerical simulations based on these methods show that the earthquake wave propagation and the surface earthquake fault formation can be reproduced to some extent. The fact that the variability due to the model uncertainty is eval-

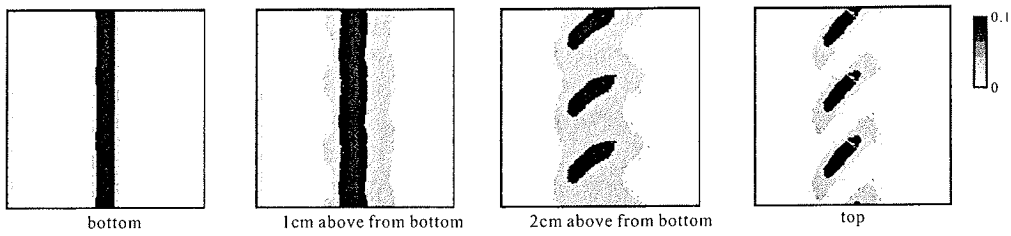

Fig. 11 Distribution of maximum shear strain on four horizontal planes from bottom to top.

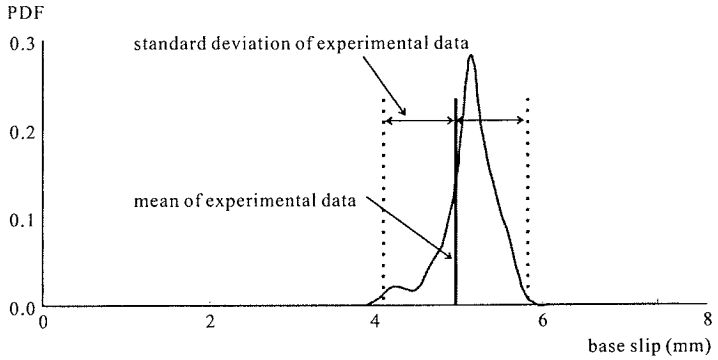

Fig. 12 Probability density function of failure with respect to base slip.

uated in efficient numerical computation should be emphasized.

In closing this paper, we mention the Monte-Carlo simulation which usually severs as an analysis method of the stochastic model. Beside that simulation of one model requires heavy numerical computation, the Monte-Carlo simulation will be *expensive* if only mean, variance, or probability density function is derived from the numerous results of the simulation. The Monte-Carlo simulation is definitely inevitable to accurately compute the probabilistic characteristics. However, such computation is not adequate only to estimate simple probabilistic characteristics of the variability. The spectral method presented here will be a suitable replacement of the Monte-Carlo simulation even if the fact that the spectral method has the limitation in the accuracy is accepted.

APPENDIX A SHARPER BOUNDING MEDIA

When the probability distribution of $c(\omega)$ is spatially uniform and isotropic, we can define bounding media which provide sharper bounds for the mean behavior of a stochastic model, applying the generalized Hashin-Shtrikman variational principle[4]. This principle is based on the equivalent inclusion method[7] that replaces a heterogeneous body B to a homogeneous body B° with eigen-stress σ_i^*. The eigen-stress is defined as the difference in stress of the two bodies, i.e., $\sigma_i^* = (c - c^{\circ})\epsilon_i$ with ϵ_i being strain in B. Thus, a stress in B° is given as $cu_{,i} + \sigma_i^*$, and the displacement is explicitly expressed in terms of Green's function of the homogeneous body.

The generalized Hashin-Shtrikman principle uses the following functional for eigen-stress:

$$K(\sigma_i^*, c) = \int_B \frac{1}{2}\sigma_i^*((c - c^{\circ})^{-1}\sigma_i^* - \epsilon_i^{\mathrm{d}} - 2\epsilon_i^{\circ})\mathrm{d}s.$$

Here, ϵ_i^{d} and ϵ_i° are strain due to the presence of σ_i^* with zero boundary displacement and strain caused by the boundary displacement $\overline{u}$ in the absence of σ_i^*, respectively. It is shown that the stationary value of K is the difference of the total strain energy stored in these two bodies, $E^{\circ} - E$ with $E^{\circ} = \int_B \frac{1}{2}c^{\circ}\epsilon_i^{\circ}\epsilon_i^{\circ}\mathrm{d}s$, and that if $c - c^{\circ}$ is positive or negative, the stationary value becomes the minimum or maximum, respectively.

The stationary value of K is approximately computed by using section-wise constant eigen-stress with Green's function, and is given as

$E^o - E^*$ where E^* is the strain energy of the body consisting of

$$c^* = \langle 1 + s(c - c^o)\rangle\langle c/(1 + p(c - c^o)\rangle^{-1},$$

and subjected to the boundary displacement $\overline{u}$. Here, p corresponds to Eshelby's tensor, and the value is 1/3. This c^* is the Hashin-Shtrikman bounds[7] for the effective moduli if $\langle(.)\rangle$ is regarded as the volume average. By choosing suitable c^o which makes $c - c^o$ positive or negative, a shaper bounding medium is determined.

APPENDIX B MULTI-SCALE ANALYSIS

Denoting by ε the ratio of the large and small length scales, the multi-scale analysis[5] first defines a fast spatial variable $\mathbf{y} = 1/\varepsilon\mathbf{x}$ and regards Young's modulus c as a function of $\mathbf{x}$ and $\mathbf{y}$; for a fixed $\mathbf{x}$, local wild change in Young's modulus is represented by the dependence of c on $\mathbf{y}$. Thus, a small region around $\mathbf{x}$, denoted by $S_\mathbf{x}$, is a domain of $\mathbf{y}$. In this setting, the homogenization method takes the singular perturbation expansion of u_i, as

$$u_i(\mathbf{x}) = u_i^{(0)}(\mathbf{x}) + \varepsilon u_i^{(1)}(\mathbf{x}, \mathbf{y}) + \cdots.$$

In view of $u_{i,j} = u_{i,j}^{(0)} + \partial u_i^{(1)}/\partial y_j + \cdots$, the second term is given as $u_i^{(1)}(\mathbf{x}, \mathbf{y}) = \chi_{ipq}(\mathbf{y}) u_{p,q}^{(0)}(\mathbf{x})$, where χ_{ipq} satisfies

$$\frac{\partial}{\partial y_i}\left(ch_{ijkl}\left(\frac{\partial \chi_{kpq}}{\partial y_l} + I_{klpq}\right)\right) = 0,$$

and a governing equation for $u_i^{(0)}$ is derived, as $(\tilde{c}_{ijkl} u_{k,l}^{(0)})_{,i} = 0$. Here, $\tilde{c}_{ijkl}$ is the effective elasticity which is defined as the volume average of $ch_{ijpq}(I_{pqkl} + \partial\chi_{pkl}/\partial y_q)$ taken over $S_\mathbf{x}$.

The multi-scale analysis assumes periodic boundary conditions for $S_\mathbf{x}$ since it is originally aimed at composite materials. Such periodicity, however, cannot be assumed for the underground. Instead of periodic boundary conditions, we use the uniform stress boundary conditions ($t_j = n_i\overline{\sigma}_{ij}$ with constant $\overline{\sigma}_{ij}$) for the upper bounding medium or uniform strain boundary conditions ($u_i = y_j\overline{\epsilon}_{ij}$ with constant $\overline{\epsilon}_{ij}$) for the lower bounding medium. This is because these boundary conditions, respectively, give the maximum and minimum total strain energy among all boundary conditions that produce the same average strain, i.e., denoting by e the strain energy density, we have

$$\int_{S_\mathbf{x}} e^\sigma \mathrm{d}v_\mathbf{y} < \int_{S_\mathbf{x}} e^g \mathrm{d}v_\mathbf{y} < \int_{S_\mathbf{x}} e^\epsilon \mathrm{d}v_\mathbf{y},$$

where superscript σ or ϵ stands for the uniform stress or strain boundary conditions and g for general (possibly mixed) boundary conditions; all these boundary conditions produce the same average strain. The above inequality is called the *universal bounds*[7] for the elastic body, since it holds for any arbitrary linearly elastic body.

REFERENCES

1) Rice, J.: New perspectives on crack and fault dynamics, in *Mechanics for a New Millennium* (Proceedings of the 20th International Congress of Theoretical and Applied Mechanics, 27 Aug - 2 Sept 2000, Chicago), eds. Aref, H. and Phillips, J.W., Kluwer, pp. 1-23, 2001.
2) Lay, T. and Wallace, C.: *Modern Global Seismology*, Academic press, 1995.
3) Ghanem, R.G. and Spanos, P.D.: *Stochastic finite elements: a spectral approach*, Springer, 1991.
4) Hori, M. and Munashinge, S.: Generalized Hashin-Shtrikman variational principle for boundary-value problem of linear and non-linear heterogeneous body, *Mechanics of Materials*, Vol. 31, pp. 471-486, 1999.
5) Hori, M. and Ichimura, T.: Macro-micro analysis for wave propagation in highly heterogeneous media - prediction of strong motion distributions in metropolis -, in *Wave 2000* (Proceedings of the International Workshop, Dec. 13-15, Bochum, Germany), eds. N. Chouw and G. Schmid, Balkema, pp. 379-398, 2000.
6) Anders, M. and Hori, M.: Stochastic finite element method for elasto-plastic body, *Int. J. Numer. Meth. Engng.*, Vol. 46, pp. 1897-1916, 1999.
7) Nemat-Nasser, S. and Hori, M.: *Micromechanics: overall properties of heterogeneous materials*, 2nd edition, North-Holland, New York, 1998.
8) Anders, M. and Hori, M.: Three-dimensional stochastic finite element method for elasto-plastic body, *Int. J. Numer. Meth. Engng.*, Vol. 51, pp. 449-478, 2001.
9) Honda, R.: Analysis of wave propagation in random media by spectral stochastic finite element method, *J. Struct. Mech./Earthquake Eng.*, JSCE, Vol. 689/I-57, pp. 321-331, 2001.
10) Fäh, D., Suhadolc, P., Mueller, P.S. and Panza, G.: A hybrid method for estimation of ground motion in sedimentary basins: quantitative modeling for Mexico City, *Bull. Seism. Soc. Am.*, Vol. 84, pp. 383-399, 1994.
11) Bardet, J.P. and Davis, C.: Engineering observations on ground motions at the Van Norman Complex after the 1994 Northridge Earthquake, *Bull. Seism. Soc. Am.*, Vol. 86, pp. 333-349, 1996.
12) Graves, R.W.: Simulating seismic wave propagation in 3D elastic media using staggered-grid finite differences, *Bull. Seism. Soc. Am.*, Vol. 86, pp. 1091-1106, 1996.
13) Kawase, H.: The cause of the damage belt in Kobe: The basin-edge effect, Constructive interference of the direct S-wave with the basin-induced diffracted/Rayleigh waves, *Seism. Res. Lett.*, Vol. 67, pp. 25-34, 1996.
14) Bao, H., Bielak, J., Ghattas, O., Kallivokas, L.F., O'Hallaron, D. R., Shewchuk, J.R. and Xu, J.: Earth-

quake ground motion modeling on parallel computers. in *Proceedings of Supercomputing '96*, 1996.
15) Komatitsch, D. and Vilotte, J.: The spectral element method: an efficient tool to simulate the seismic response of 2D and 3D geological structures, *Bull. Seism. Soc. Am.*, Vol. 88, pp. 368-392, 1998.
16) Ortiz-Aleman, C., Sanchez-Sesma, F.J., Rodriguez-Zuniga, J.L. and Luszon, F.: Computing topographical 3D site effects using a fast IBEM/conjugate gradient approach, *Bull. Seism. Soc. Am.*, Vol. 88, pp. 393-399, 1998.
17) Inoue, T. and Miyata, T.: 3D simulation of near-field strong ground motion based on dynamic loading, *Bull. Seism. Soc. Am.*, Vol. 88, pp. 1445-1456, 1998.
18) Furumura, T. and Koketsu, K.: Specific distribution of ground motion during the 1995 Kobe earthquake and its generation mechanism, *Geophys. Res. Lett.*, Vol. 25, pp. 785-788, 1998.
19) Pitarka, A.: 3D elastic finite-difference modeling of seismic motion using staggered grids with non-uniform spacing, *Bull. Seism. Soc. Am.*, Vol. 89, pp. 54-68, 1999.
20) Fujiwara, H.: The fast multi-pole method for solving integral equations of three-dimensional topography and basin problems, *Geophys. J. Int.*, Vol. 140, pp. 198-210, 2000.
21) Irikura, K.: Prediction of strong acceleration motions using empirical Green's function, *Proc. 7th Japan Earthquake Engineering Symposium*, pp. 151-156, 1986.
22) Kikuchi, M. and Ishida, M.: Source retrieval for local earthquakes with broadband records, *Bull. Seism. Soc. Am.*, Vol. 83, pp. 1885-1870, 1993.
23) Aki, K.: Local site effect on ground motion. in *Earthquake Engineering and Soil Dynamics II: Recent Advances in Ground-Motion Evaluation*, ed. J.L.V. Thun, ASCE, 1988.
24) Yamanaka, H., Sato, H., Kurita, K. and Seo, K.: Array measurements of long-period microtremors in southwestern Kanto Plain, Japan, *Zisin*, Vol. 51, pp. 355-365, 1999 (in Japanese).
25) *Proceedings of Seismic Fault-induced failures* - Possible remedies for damage to urban facilities - (ed. By K. Konagai), JSPS Research Project 2000, 2001.
26) Bray, J.D., Seed, R.B. and Seed, H.B.: Earthquake fault rupture propagation through soil, *J. Geotech. Eng.*, ASCE, Vol. 120, No. 3, pp. 543-561, 1994.
27) Ke, T-C. and Bray, J.D.: Modeling of particulate media using discontinuous deformation analysis, *J. Eng. Mech.*, ASCE, Vol. 121, No. 11, pp. 1234-1243, 1995.
28) Roth, W.H., Kalis, G., Papastamatiou, O. and Cundall, P.A.: Numerical modeling of fault propagation in soils, in *Proc. 4th Int. Conf. on Num. Meth. Geomech.*, pp. 487-494, 1982.
29) Cole, D.A. and Lade, P.V.: Influence zones in alluvium over dip-slip fault, *J. Geotech. Eng.*, ASCE, Vol. 110, No. 5, pp. 599-615, 1984.
30) Tani, K. and Ueta, K.: Shape and location of discontinuity in sand induced by fault displacement in bed rock, in *Proc. 26 Japan National Conf. on Geotech. Eng.*, JSGE, pp. 1185-1188, 1991 (in Japanese).
31) Taniyama, T. and Watanabe, H.: Deformation of sandy deposits by reverse faulting, *J. Struct. Mech./Earthquake Eng.*, JSCE, Vol. 591/I-43, pp. 313-325, 1998.
32) Ohuchi, M., Abe, S.. Kusakabe, H. and Hagiwara, T.: Development of shear band and particle crushing observed in in - situ loading tests on a sedimented sand, JSCE, Vol. 487/III-26, pp: 207-216, 1994.
33) Proposal of simplified design method for buried pipes crossing earthquake fault, *J. Struct. Mech./Earthquake Eng.*, JSCE, Vol. 668/I-54, pp. 197-194, 2001.
34) Oguni, K., Hori, M. and Ikeda, K.: Analysis on evolution pattern of periodically distributed defects, *International Journal of Solids and Structures*, Vol. 34, No. 25, pp. 3259-3772, 1997.
35) Hori, M. and Vaikuntan, N.: Rigorous formulation of crack path in two-dimensional elastic body, *Mechanics of Materials*, Vol. 26, pp. 1-14, 1997.
36) Hori, M. and Vaikuntan, N.: Analysis of the initiation of periodically distributed defects, *Int. J. Plasticity*, Vol. 14, No.8, pp. 673-688, 1998.

(Received September 31, 2002)